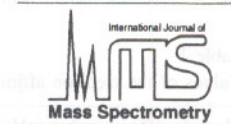




ELSEVIER



Electron attachment cross sections and negative ion states of SF₆

Loucas G. Christophorou* and James K. Olthoff

Electricity Division, Electronics and Electrical Engineering Laboratory, National Institute of Standards and Technology, Gaithersburg, MD 20899-8113, USA

Received 9 February 2000; accepted 23 March 2000

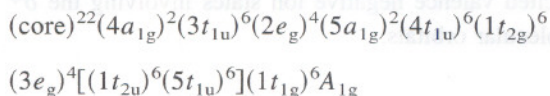
Abstract

A comprehensive and critical assessment of published data on the total, dissociative and nondissociative electron attachment cross sections for SF₆ allowed us to recommend or suggest room temperature values for these cross sections over an energy range from 0.0001 eV to 15 eV. The total electron attachment cross section is dominated by the formation of SF₆⁻ below ~0.2 eV, by the formation of SF₅⁻ between ~0.3 eV and 1.5 eV, and by the formation of F⁻ beyond ~2.0 eV. This work, along with electron scattering and theoretical data, allowed us also to identify the energies and symmetry assignments of the negative ion states of SF₆ below ~15 eV. (Int J Mass Spectrom 205 (2001) 27–41) © 2001 Elsevier Science B.V.

Keywords: Cross sections; Electron attachment; Negative ions; SF₆; Sulfur hexafluoride

1. Negative ion states of SF₆

The SF₆ molecule belongs to the point group O_h. Its ground-state valence electron configuration is (see, for example, Refs. [1] and [2]):



although there are still some questions as to the energetic sequence of the various orbitals (for instance, the (5t_{1u}) and (1t_{2u}) orbitals are nearly degenerate and their ordering unresolved). The four lowest empty (valence) orbitals of SF₆ are [2,3]

(6a_{1g})⁰(6t_{1u})⁰(2t_{2g})⁰(4e_g)⁰. Calculations for the octahedral symmetry (O_h) of SF₆⁻ (e.g., see Refs. [4–7]) have shown that the S–F antibonding character of the highest occupied totally symmetric nondegenerate 6a_{1g} molecular orbital of SF₆⁻ results in a substantial increase of the S–F bond in SF₆⁻ compared to neutral SF₆. Although a number of authors (e.g., Refs. [8–10]) have considered electron capture into degenerate molecular orbitals of lower symmetry than a_{1g}, calculations for a lower symmetry configuration (e.g., see Gutsev [11,12] and Richman and Banerjee [13]) showed the O_h octahedral structure to be the most stable.

Although there has been widespread unanimity that SF₆ attaches thermal and near-thermal energy electrons with a very large cross section forming SF₆⁻, and that the SF₆ molecule must thus have a positive electron affinity, up until recently there has been no unanimity regarding the size of its electron affinity.

* Corresponding author.

Dedicated to Professor Aleksandar Stamatovic on the occasion of his 60th birthday.

Table 1
Values of the electron affinity of the SF₆ molecule reported since 1983

Electron affinity value (eV)	Reference	Comments
0.0–1.49 [0.76] ^a	14	Range of 20 values listed in Ref. 14, which were reported prior to 1983
1.05 ± 0.1	15	Energetics of electron transfer reactions
1.15 ± 0.15	16	Thermal electron attachment studies
1.07 ± 0.07 ^b	17	Thermal electron attachment studies
1.19	6	Calculation
1.3–1.4	7	Calculation
1.06	18	Calculation
3.44	12	Calculation
3.46	11	Calculation
Recommended value: 1.06 eV		

^a Average of the values listed in Ref. 14 excluding the lowest and the highest values listed.

^b This value is a refinement of their earlier result [16].

This, in spite of the fact that by 1983 there were at least 20 reported values for this quantity [14]. These vary from ~0.0 eV to ~1.5 eV. Their average (excluding the lowest and the highest value listed in Ref. [14]) is 0.76 eV. This average value and other values reported since 1983 are listed in Table 1. We take the average of the two most recent and widely accepted values determined in Refs. [15] and [17] to be our presently recommended value of 1.06 eV for the electron affinity of the SF₆ molecule.

In addition to the electron attachment resonance at ~0.0 eV, electron attachment and electron scattering experiments and calculations, have shown the existence of several negative ion states at energies below ~15 eV. The energies of these states, as determined by the positions of the maxima in the measured electron attachment cross sections, measured electron scattering cross sections, and calculated cross sections, are listed in Table 2. Also listed in Table 2 are possible symmetry assignments. The experimental and the calculated values are plotted in Fig. 1. The electron attachment data for each resonance exhibit a considerable spread partly because these data involve a number of different fragment negative ions. The energy range for each resonance as determined by the electron attachment studies, extends to lower energies than the respective energy range determined by the electron-scattering studies. This difference is especially large for the 7.0 eV resonance and can be attributed to the competition between dissociation and

autodetachment of SF₆^{-*} in the former case. It is interesting to note that although electron attachment studies and theory indicate a resonance at ~9 eV, none of the electron scattering investigations show any evidence of it.

The last column in Fig. 1 gives the recommended energy positions of the SF₆ resonances as determined by considering only the electron scattering data, along with their symmetry assignments. The energy positions of the lowest negative ion states of the SF₆ molecule and their symmetries are: ~0.0 eV (*a*_{1g}), 2.5 eV (*a*_{1g}), 7.0 eV (*t*_{1u}), and 11.9 eV (*t*_{2g}). It should be noted that the adiabatic position of the ~0.0 eV negative ion state is at -1.06 eV [= -|EA(SF₆)|]. Other negative ion states are indicated at ~17 eV and higher energies (see Table 2). The resonances at ~27 eV and ~50 eV (Table 2) can be assigned as core-excited valence negative ion states involving the σ* molecular orbitals.

2. Electron attachment cross sections for SF₆

2.1. Cross sections for the formation of SF₆⁻, SF₅⁻, SF₄⁻, SF₃⁻, SF₂⁻, F₂⁻, and F⁻

Electron attachment to SF₆ leads to the formation of both parent (SF₆⁻) and fragment (SF₅⁻, SF₄⁻, SF₃⁻, SF₂⁻, F₂⁻, and F⁻) negative ions. The room temperature experimental data on the cross sections for the

Table 2
Negative ion states of SF₆

Energy position (eV)	Type of study	Symmetry/orbital	Reference
~0.0	Many electron attachment studies		
0.38	SF ₅ ⁻ from SF ₆		19-21
0.5 ± 0.1	SF ₅ ⁻ from SF ₆		22
~0.1	Excitation function of ν ₁	A _{1g}	23
~0.1	Vibrational excitation by electron impact		24
~0.0	Multiple scattering calculation	a _{1g}	25
2.0	F ₂ ⁻ from SF ₆		20
2.2	F ₂ ⁻ from SF ₆		26
2.4	F ₂ ⁻ from SF ₆		27 ^a
2.6	F ⁻ from SF ₆		20
2.8	F ⁻ from SF ₆		27
2.8	F ⁻ from SF ₆		26
~2.9	F ⁻ from SF ₆		28
2.3	Total electron scattering cross section	a _{1g}	29
2.5	Total electron scattering cross section	A _{1g}	30
2.5	Total electron scattering cross section	a _{1g}	31
2.52 ± 0.15	Trochoidal derivative spectrum	a _{1g}	32
2.56 ± 0.15	Total electron scattering cross section	a _{1g}	32
2.7	Angular dependence of vibrationally elastic electron scattering	a _{1g}	33
2.1	Multiple scattering calculation	a _{1g}	25
3.30	Multichannel calculation with close-coupling	A _{1g}	34
4.4	F ₂ ⁻ from SF ₆		20
4.8	F ₂ ⁻ from SF ₆		27
4.8	F ₂ ⁻ from SF ₆		26
5.0	SF ₄ ⁻ from SF ₆		26
5.1	F ⁻ from SF ₆		20
5.2	F ⁻ from SF ₆		27
5.3	F ⁻ from SF ₆		26
5.4	SF ₄ ⁻ from SF ₆		20
5.4	SF ₄ ⁻ from SF ₆		27
~5.4 ^b	F ⁻ , F ₂ ⁻ , and SF ₄ ⁻ from SF ₆		28
5.7 ± 0.1	F ⁻ from SF ₆		22
6.0 ± 0.1	SF ₄ ⁻ from SF ₆		22
6.7	Total electron scattering cross section	t _{1g}	29
7.0	Total electron scattering cross section	t _{1u}	31
7	Angular dependence of vibrationally elastic electron scattering	t _{1u}	33
7	Total electron scattering cross section	t _{1u}	30
7.01 ± 0.16	Trochoidal derivative spectrum	t _{1u}	32
7.05 ± 0.10	Total electron scattering cross section	t _{1u}	32
7.2	Elastic electron scattering cross section	t _{1u}	35
7.2	Multiple scattering calculation	t _{1u}	25
8.8	F ⁻ from SF ₆		20
8.9	F ⁻ from SF ₆		27
9.3 ± 0.1	F ⁻ from SF ₆		22
9.4	F ⁻ from SF ₆		26
9.4	SF ₃ ⁻ from SF ₆		20
8.7; 9.1	Multiple scattering calculations	T _{1u}	36
9.85	Multichannel calculation with close-coupling	T _{1u}	34

(continued on next page)

Table 2 (continued)

Energy position (eV)	Type of study	Symmetry/orbital	Reference
11.2	F ₂ ⁻ from SF ₆		20
11.2	SF ₃ ⁻ from SF ₆		27
11.3	SF ₃ ⁻ from SF ₆		26
11.3	F ⁻ from SF ₆		20
11.5	F ⁻ from SF ₆		27
11.6	F ⁻ from SF ₆		26
11.6	F ₂ ⁻ from SF ₆		26
11.7	F ₂ ⁻ from SF ₆		20
11.8 ± 0.1	F ⁻ from SF ₆		22
12.0	SF ₂ ⁻ from SF ₆		20
12.3	SF ₂ ⁻ from SF ₆		26
13.0	SF ₂ ⁻ from SF ₆		27
11.87 ± 0.10	Total electron scattering cross section	t _{2g}	32
11.88 ± 0.07	Trochoidal derivative spectrum	t _{2g}	32
11.9	Total electron scattering cross section	t _{2g}	31
11.9	Total electron scattering cross section	t _{2g}	29
12	Total electron scattering cross section	t _{2g}	30
12	Elastic electron scattering cross section	t _{2g}	35
12	Elastic and vibrationally inelastic electron-impact excitation		37
11	Multiple scattering calculation	T _{1u}	38
11.0; 11.8; 13.7	Multiple scattering calculation	T _{2g}	36
12.7	Multiple scattering calculation	t _{2g}	25
13.10	Multichannel calculation with close coupling	T _{2g}	34
16.8	Total electron scattering cross section		31
17	Multiple scattering calculation of total cross section for elastic electron scattering	T _{2g}	38
23–24	Angular distribution of photoelectrons		1
24	Multiple scattering calculation	E _g	38
27.0	Multiple scattering calculation	e _g	25
27.0	Multichannel calculation with close coupling	e _g	34
27.1; 28.3; 28.6	Multiple scattering calculation	E _g	36
28.84	Multichannel calculation within close coupling	E _g	34
25–55 ^c	Total electron scattering cross section	e _g	32

^a The values of Lehman [27] given in this table have been deduced from his figures and were reduced by 0.6 eV as discussed in the text.

^b Main resonance.

^c Possibly one or more resonances in this energy range.

formation of each of these negative ions are presented and discussed in this section. The measured cross sections for the various negative ions formed by electron impact on SF₆ show that the parent negative ion SF₆⁻ is formed only at low electron energies (below ~0.3 eV), and that the fragment negative ions are formed via a number of negative ion resonances located between 0 eV and ~15 eV.

2.1.1. SF₆⁻

The stable parent negative ion SF₆⁻ produced at zero and near-zero electron energy is initially formed

as a metastable SF₆^{-*} ion which subsequent to its formation is stabilized by collision or radiation. Its autodetachment lifetime, τ_a, under collision-free conditions has been found to be >1 μs (between 10 μs and 68 μs) using time-of-flight (TOF) mass spectrometric measurements [39–44]. Similar measurements using ion cyclotron resonance (ICR) techniques found the lifetime of SF₆^{-*} to be much longer, in the ms range [45–47]. This is not surprising, since a number of studies (e.g., see Refs. [43,44,48]) have shown that the autodetachment lifetime of a number of polyatomic long-lived transient negative ions depends on

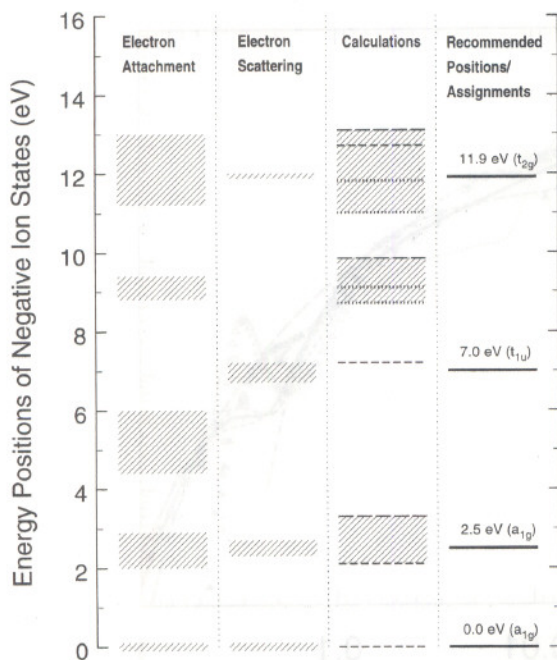


Fig. 1. Negative ion states of the SF_6 molecule as determined by electron attachment measurements, electron scattering measurements, and calculations (--- [25]; -- [34]; ... [36]). Shaded areas represent the range of measured resonant energies. The last column gives the recommended average positions and assignments (see text). Note that the adiabatic position of the ~ 0.0 eV negative ion state is at -1.06 eV [$= -|\text{EA}(\text{SF}_6^-)|$].

the experimental conditions (kinetic energy of the captured electron, internal energy of the electron capturing molecule, and hence the gas temperature), and the electron energies are normally much lower in ICR experiments than in TOF experiments. Whereas no effect of the attaching electron's energy on the τ_a of SF_6^{*-} has been reported, such energy dependence has been found for other transient anions [43,49–53]. Furthermore, Delmore and Appelhans [54] observed an increase of $\sim 33\%$ in the τ_a of the metastable SF_6^{*-} ion when the temperature of their ion source was decreased from $\sim 475\text{K}$ to $\sim 375\text{K}$, which they attributed to the contribution of various excited states to the autodetachment process. It has also been shown [46] that the τ_a of SF_6^{*-} in the ICR spectrometer varies with the observation time of the experiment, thus accounting [46,55] for radiative and collisional cooling of SF_6^{*-} .

Besides the formation of SF_6^- by direct attachment of low-energy electrons, SF_6^- can also be formed indirectly by relatively higher energy electrons when these electrons lose “all” of their energy to inelastic electron scattering and are then picked up efficiently as “zero-energy” electrons by the SF_6 molecules. Indeed, this is the basis of the so-called “ SF_6^- threshold-electron excitation technique” used to locate negative-ion states and excited electronic states, especially optically forbidden states, of neutral molecules (e.g., Refs. [56–59]).

Many early studies (e.g., Refs. [27,40,56,57,60–65]) showed that SF_6^- is formed at ~ 0.0 eV with a very large cross section. These studies also indicated that the shape of the measured cross section for the formation of SF_6^- is instrumental, that is, the SF_6^- resonance is narrower than the energy spread of the electron pulse used to measure it. This narrowness of the SF_6^- resonance is largely responsible for the large uncertainty and the large spread in the early published values of the electron attachment cross section, $\sigma_{a,\text{SF}_6^-}(\epsilon)$, for formation of SF_6^- at thermal and near-thermal energies. There have been a number of subsequent (room temperature) studies using both conventional electron beam [20,66,67] and electron swarm [19,68–72] techniques. Additionally, newer very high resolution and very low energy electron beam techniques have been used to provide accurate values of the absolute cross section for the attachment of free electrons to SF_6 to form SF_6^- in the ~ 1 eV to the micro-eV range [73–82]. Besides these methods, information on σ_{a,SF_6^-} has been provided in the thermal and subthermal electron energy range by another new technique using “bound-electron” capture in collisions of SF_6 with high-Rydberg atoms [78,83–99]. The results obtained by these methods are complementary to those obtained by direct “free” electron-impact methods. The cross-section data determined by these methods are plotted in Fig. 2 and are briefly discussed below.

Data obtained by conventional electron-swarm and electron-beam techniques. The swarm data plotted in Fig. 2 [19,69–72] have been unfolded from the total electron attachment rate-constant measurements made

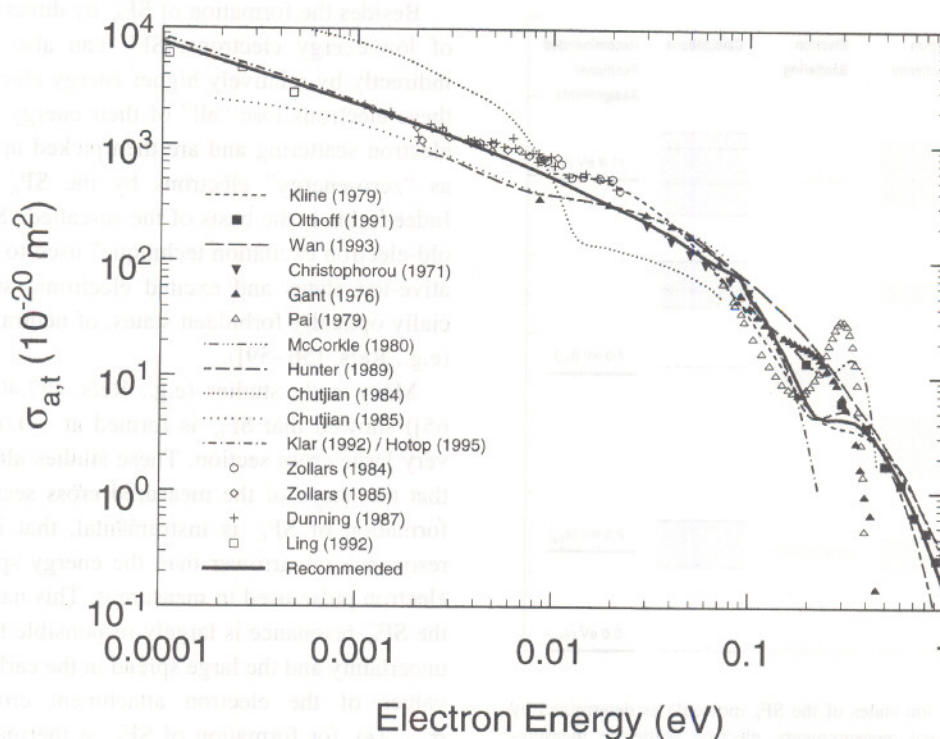


Fig. 2. Measured total electron attachment cross section, $\sigma_{a,t}(\epsilon)$, for SF_6 as a function of the electron energy, for free electrons and for electrons bound in high-Rydberg states of atoms (see text). Below ~ 0.1 eV this cross section is about equal to that, $\sigma_{a,\text{SF}_6^-}(\epsilon)$, for the production of SF_6^- . Conventional electron-beam data: - - - [20]; ■ [66]; -- [67] Swarm-unfolded data: ▼ [19]; ▲ [69]; △ [70]; -.-.- [71]; — [72]. TPISA technique: [76] (data normalized to the thermal electron attachment rate constant value of Crompton and Haddad [100]); ... [77] (data normalized to the swarm-unfolded cross section of McCorkle et al. [71]). LPA technique: -.- [79,101]. High-Rydberg data: ○, Xe*(nf) [86]; ◇, Rb*(ns, nd) [87]; +, Rb*(ns, nd), K*(nd), Xe*(nf) [89]; □, K*(np) [94]. —, recommended values.

in mixtures of SF_6 with N_2 buffer gas. They are therefore total cross sections. However, since below ~ 0.1 eV SF_6^- is by far the predominant negative ion, in the energy region below ~ 0.1 eV these cross sections give the value of σ_{a,SF_6^-} . It is difficult to assess the uncertainty of these cross-section data. Although the rate constant measurements are expected to have an uncertainty around $\pm 10\%$, the cross section values have a larger uncertainty. Similarly, the electron-beam data have a large uncertainty at low energies. Kline et al. [20] used the retarding-potential-difference method in their experiments and their energy resolution was typically between 80 meV to 100 meV. Their cross section below ~ 0.1 eV is therefore instrumental. The measurements of Olthoff et al. [66] and Wan et al. [67] are for the total electron

attachment cross section and were made using a trochoidal monochromator ($T = 328\text{K}$). They have a quoted uncertainty of $\pm 15\%$ above 1 eV and a larger uncertainty below this energy, which perhaps increases to $\pm 50\%$ at 0.2 eV.

Data obtained from very-high resolution, very-low energy electron-beam techniques. Two such techniques have been developed, one by Chutjian and collaborators [73–77] and the other by Hotop and collaborators [78–82]. The two techniques are similar in principle. The technique of the former group uses VUV photoionization of rare-gas atoms mixed with SF_6 to generate in situ photoelectrons of well defined and variable energy. It is referred to as the threshold-photoelectron-spectroscopy-by-electron-attachment

(TPSA) technique and provides relative cross sections for electron energies in the range from a few meV to 150 meV with electron-energy resolution between 6 meV and 8 meV (full-width-at-half-maximum, FWHM) [76]. The energy dependence of the cross section is obtained using convolution techniques and the absolute value is determined by normalization to electron swarm data. The data of Chutjian et al. [76] were normalized to the thermal electron attachment rate constant ($2.27 \times 10^{-7} \text{ cm}^3 \text{ s}^{-1}$) of Crompton and Haddad [100], while the data of Chutjian and Alajajian [77] were normalized to the swarm-unfolded cross-section data of McCorkle et al. [71].

The technique of Hotop and collaborators is referred to as the laser-photoelectron-attachment (LPA) method and is based on the controlled production of variable-energy photoelectrons using lasers to photoionize a well-collimated beam of metastable Ar^* ($4s^3P_2$) atoms from a differentially-pumped DC discharge source in a field-free region. The resulting negative ions are then detected by application of pulsed electric fields [79]. This technique has permitted the energy dependence of the cross section to be measured directly with sub-meV resolution. The values measured by Hotop and collaborators [79,101] for σ_{a,SF_6^-} in the range 0.0001 eV to ~ 0.230 eV are shown in Fig. 2. These cross-section values were obtained by normalization to the thermal ($T = 300\text{K}$) rate-constant measurement of Crompton et al. [100,102]. It should be emphasized that the cross section of Hotop et al. in Fig. 2 is only for the formation of SF_6^- , whereas the rest of the data above 0.1 eV are total electron attachment cross sections.

Data obtained from high-Rydberg atom bound-electron capture methods. A number of investigators, foremost the group at Rice University, have used beams of atoms excited in high-Rydberg states, $\text{A}^{**}(nl)$, and measured the rate constant for the reaction

$$\text{A}^{**}(nl) + \text{SF}_6 \rightarrow \text{A}^+ + \text{SF}_6^- \quad (1)$$

down to $\sim 4 \mu\text{eV}$ [99]. In almost all such investigations, $\text{A}^{**}(nl)$ is a rare-gas or an alkali-metal atom in a Rydberg state with principal quantum number n and

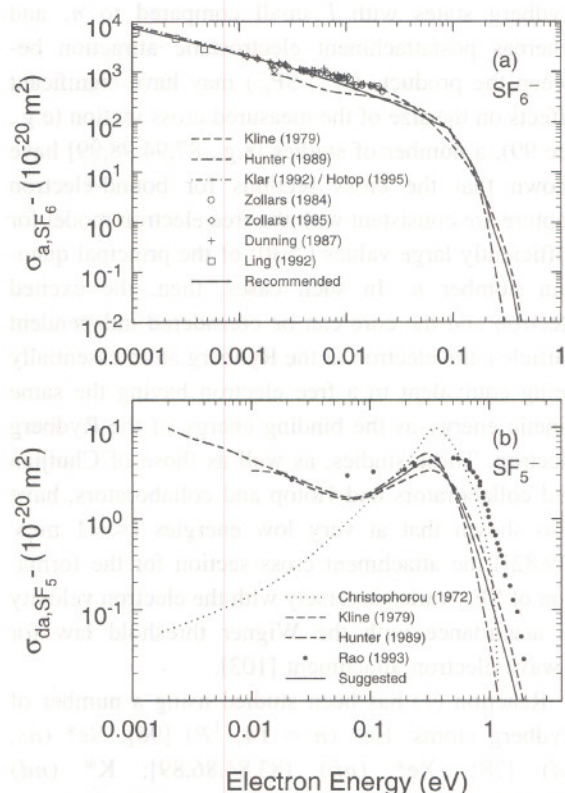


Fig. 3. (a) Selected measurements on the electron attachment cross section, $\sigma_{a,\text{SF}_6^-}(\epsilon)$, for the formation of SF_6^- from SF_6 as a function of the electron energy (see text). --- [20]; -- [72]; -·- [79,101]; ○ [86]; ◇ [87]; + [89]; □ [94]; —, recommended values. (b) Selected measurements on the dissociative electron attachment cross section, $\sigma_{\text{da},\text{SF}_5^-}(\epsilon)$, for the formation of SF_5^- from SF_6 as a function of the electron energy. . . . [19]; --- [20]; -·- [72]; ● [26]; — suggested data.

angular momentum quantum number l . In these studies the rate constant $k_{a,\text{be}}$ for the formation of SF_6^- is measured as a function of the principal quantum number n , or as a function of the effective principal quantum number $n^*(= n - \delta_l)$, where δ_l is the l -dependent quantum defect). From these rate-constant data, the cross section for bound-electron capture, $\sigma_{a,\text{be}}(\nu)$, is determined via the relation

$$\sigma_{a,\text{be}}(\nu) = k_{a,\text{be}}(n^*)/\nu_{\text{rms}} \quad (2)$$

where ν_{rms} is the root-mean-square velocity of the Rydberg electron. While a number of authors [e.g., see 97,99] have shown Eq. (2) to be inappropriate for

Rydberg states with l small compared to n , and whereas postattachment electrostatic attraction between the products (A^+ , SF_6^-) may have significant effects on the size of the measured cross section (e.g., see 99), a number of studies [e.g., 87,94,98,99] have shown that the cross sections for bound-electron capture are consistent with the free electron model for sufficiently large values (>30) of the principal quantum number n . In such cases, then, the excited electron and the core can be considered independent particles, the electron in the Rydberg atom essentially being equivalent to a free electron having the same kinetic energy as the binding energy of the Rydberg electron. These studies, as well as those of Chutjian and collaborators and Hotop and collaborators, have also shown that at very low energies ($<\sim 1$ meV [79,82]) the attachment cross section for the formation of SF_6^- varies inversely with the electron velocity in accordance with the Wigner threshold law for s-wave electron attachment [103].

Reaction (1) has been studied using a number of Rydberg atoms: He^* ($n = 14$, 1P) [96]; Ne^* (ns , nd) [78]; Xe^* (nf) [83,84,86,89]; K^* (nd) [88,89,91]; K^* (np) [94]; Na^* (np) [90]; Rb^* (ns , nd) [87,89]; and Cs^* (ns , np , nd) [92]. The results of these high-Rydberg-atom studies on $\sigma_{a,be}(\nu)$ are plotted in Fig. 2.

The wide spread in the data in Fig. 2 and the many factors that can affect them which are often not clearly discerned, makes the deduction of a recommended cross section $\sigma_{a,t}(\epsilon)$ for SF_6 from the data in Fig. 2 difficult. However, since at energies below ~ 1.5 eV SF_6^- and SF_5^- are the only negative ions produced by electron attachment to SF_6 , we determined the recommended cross section $\sigma_{a,t}(\epsilon)$ for SF_6 up to ~ 1 eV, shown by the solid line in Fig. 2, by summing our recommended cross section for SF_6^- and our suggested cross section for SF_5^- . These have been determined separately as shown below.

The determination of the recommended cross section, $\sigma_{a,SF_6^-}(\epsilon)$, for the formation of SF_6^- was made by considering the data in Fig. 3a. The line (- - -) represents the measurements of Hotop and collaborators [79,101] obtained using the LPA technique, and the lines (— —) and (- - -) are the cross sections for

the production of only SF_6^- as obtained respectively from electron-swarm-based measurements by Hunter et al. [72] and from electron-beam-based measurements by Kline et al. [20]. The points shown in the figure are the bound-electron attachment cross sections (of Refs. [86,87,89,94]) for energies below ~ 0.005 eV for which the data are generally free of the complications discussed earlier. At these low energies, the cross section values of Hotop and collaborators are in excellent agreement with the bound-electron attachment measurements. On the high-energy side, the cross section of Hotop et al. drops off abruptly at the onsets of ν_1 , ν_3 , and $2\nu_1$ vibrational excitations (see discussion in Refs. [79] and [101]). It is in overall agreement with the data of Hunter et al. and Kline et al. considering the precipitous decline in the magnitude of the cross section with increasing energy in this energy range. The measurements of Hotop et al. in the energy range 0.0001 eV to 0.230 eV, the bound-electron attachment data below 0.005 eV, and the data of Hunter et al. and Kline et al. above 0.2 eV were combined to yield the solid line in Fig. 3(a), which represents our recommended values for $\sigma_{a,SF_6^-}(\epsilon)$ in the energy range from 0.0001 eV to 0.40 eV.

The other free-electron data in Fig. 2 were not considered for various reasons:

- (1) The data of Chutjian and collaborators are indirect measurements both in absolute magnitude and energy dependence. Also, according to Chutjian [104] part of the disagreement between the data they obtained using the TPSA technique and the data obtained using the LPA and the bound-electron attachment methods are due to the effects of stray fields on the TPSA measurements.
- (2) The electron beam data of Olthoff et al. [66] and Wan et al. [67] do not show the enhancement at ~ 0.4 eV due to SF_5^- born out by all other electron beam and electron swarm studies and they have a large stated uncertainty.
- (3) From the various swarm-based cross sections we considered only the most recent data of Hunter et al. [72] since these measurements were more accurate and more extensive than the previous ones, and

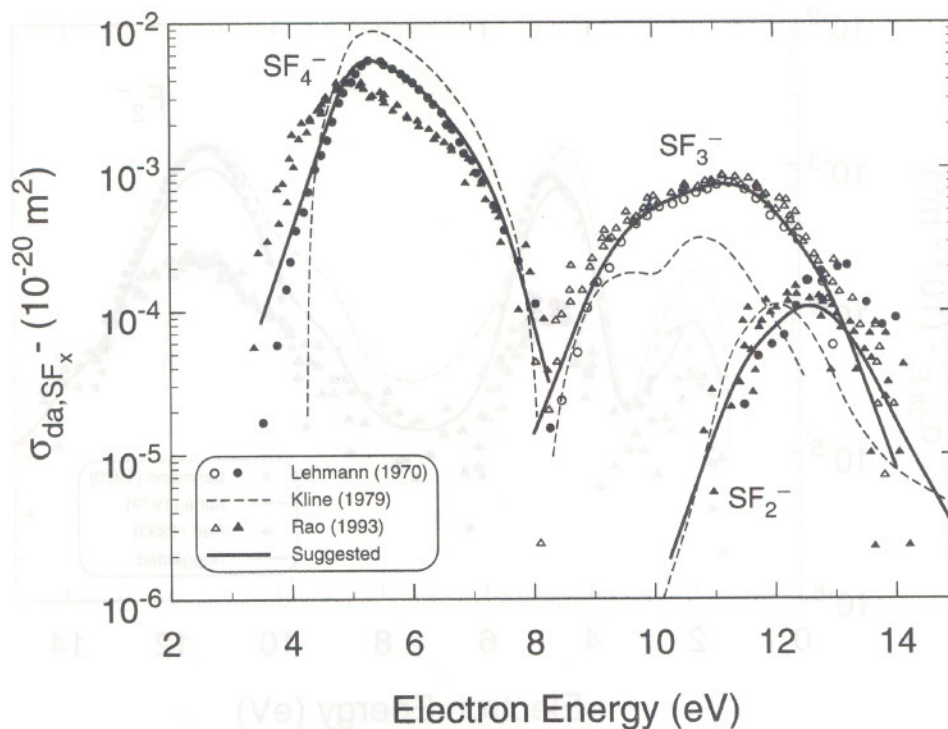


Fig. 4. Cross sections for the formation of SF_4^- , SF_3^- and SF_2^- by dissociative electron attachment to SF_6 as a function of the electron energy \bullet , \circ [27]; --- [20]; \blacktriangle , \triangle [26]; —, suggested values.

since more recent cross sections were employed in the determination of the electron energy distribution functions used to obtain the swarm-based cross sections from the measured rate constants.

2.1.2. SF_5^-

A number of electron-beam studies [19–22,26,28,105], have shown that at energies below ~ 1.5 eV, SF_5^- is produced via the dissociative electron attachment reaction



with maxima at ~ 0.0 eV and 0.38 eV. It has been shown by Chen and Chantray [21] that the first peak at ~ 0.0 eV is very sensitive to gas temperature and that the second peak at 0.38 eV is rather independent of gas temperature. Interestingly, Matejcik et al. [105] have recently found that the first peak at 0.0 eV disappears at temperatures below ambient.

In Fig. 3(b) the published values are compared of the cross section, $\sigma_{da,SF_5^-}(\epsilon)$, for the formation of SF_5^- by low-energy electron impact on SF_6 as a function of electron energy: electron-swarm-normalized data [19,72] and electron-beam data [20,26]. In none of these studies were uncertainties quoted. As can be seen from Fig. 3(b) there are large differences in the cross section data for the production of SF_5^- from SF_6 , especially below ~ 0.1 eV. The latter may partly be due to the varied effects of temperature on the formation of SF_5^- at the low energies [e.g., see 81, 106,107] which are still unresolved. For this reason, we suggest data for the cross section, $\sigma_{da,SF_5^-}(\epsilon)$, for the formation of SF_5^- by electron attachment to SF_6 , down to only 0.1 eV. These suggested data are shown in Fig. 3(b) by the solid line which was obtained by a least squares fit to the data from Refs. [20] and [72]. The data of Rao and Srivastava [26] were excluded since they exhibit a large energy uncertainty due to

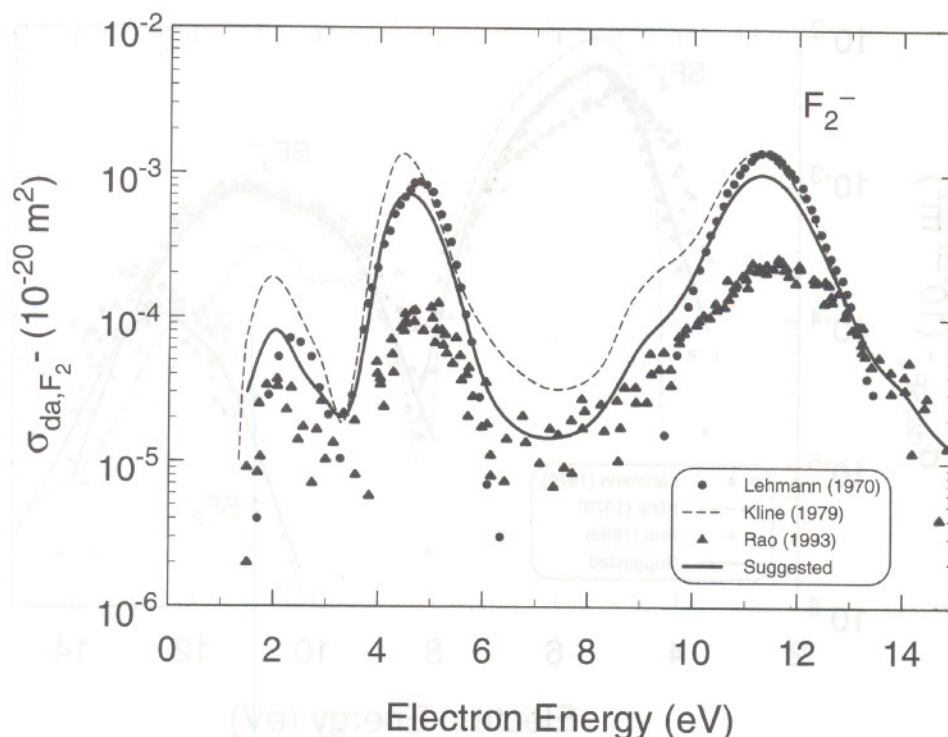


Fig. 5. Cross section for the formation of F_2^- by dissociative electron attachment to SF_6 as a function of the electron energy. ● [27]; --- [20]; ▲ [26]; —, suggested data.

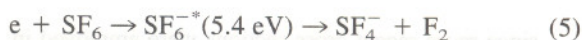
the difficulty of obtaining accurate values from the sharp SF_5^- peak shown in the graph of their paper. It should be noted, that at room temperature the contribution of SF_5^- to the total electron attachment cross section below ~ 0.1 eV is small.

2.1.3. SF_4^- , SF_3^- and SF_2^-

These ions are generated mostly through negative-ion states located at progressively higher energies (Table 2). The SF_4^- fragment is generated from a broad resonance between 4 eV and ~ 8 eV. Harland and Thynne [22] attributed the production of this ion to the reaction



and reported the cross section maximum for this ion to be at (6.0 ± 0.1) eV. In contrast, Fenzlaff et al. [28], although not excluding reaction (4) for the formation of SF_4^- , attributed its formation at least on the high energy side of the resonance, to the reaction



with a threshold at (2.8 ± 0.1) eV and a peak at 5.4 eV.

Cross sections for all three fragment negative ions have been measured at room temperature by Lehmann [27], Kline et al. [20] and Rao and Srivastava [26] and are shown in Fig. 4. Kline et al. established the magnitudes of the cross sections by measuring the various positive-ion cross sections and calibrating their sum with the total ionization cross section measurements of Rapp and Englander-Golden [108]. In Fig. 4 the data of Lehmann were shifted to lower energies by 0.6 eV, as suggested by Kline et al. In the experiments of Kline et al. the effective electron energy resolution was between 0.08 eV to 0.1 eV with an estimated uncertainty of the electron energy scale of ± 0.1 eV. Rao and Srivastava [26] measured peak cross section values for SF_4^- , SF_3^- , and SF_2^- , respectively equal to 4.0×10^{-19} cm², 8.8×10^{-20} cm²

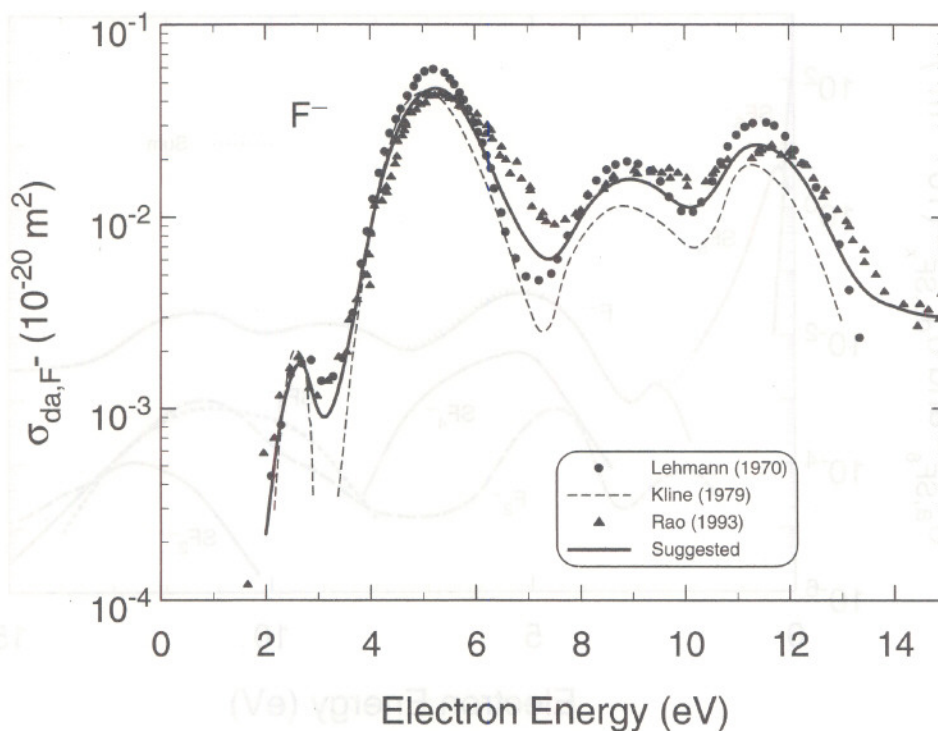


Fig. 6. Cross section for the formation of F^- by dissociative electron attachment to SF_6 as a function of the electron energy. ● [27]; --- [20]; ▲ [26]; — suggested data.

and $1.3 \times 10^{-20} \text{ cm}^2$. The data of Rao and Srivastava in Fig. 4 were taken off their plots and were put on absolute scale using these peak cross section values. With the applied shift in the Lehmann data, the agreement in the magnitude and energy dependence of the cross section for these three ions as measured by Lehmann and by Rao and Srivastava is reasonable. The solid lines shown in the figure for each negative ion fragment represent our respective suggested cross section values. They were obtained by a least squares fit to all three sets of measurements, except for the case of the SF_3^- ion, where only the data of Refs. 26 and 27 were considered.

2.1.4. F_2^-

The F_2^- ion is produced in the energy range from approximately 1 eV to 14 eV. Its cross section shows maxima located at ~ 2.2 eV, ~ 4.7 eV and ~ 11.5 eV. Figure 5 compares the room temperature cross section

measurements of Lehmann [27], Kline et al. [20] and Rao and Srivastava [26]. The data of Lehmann were again shifted to lower energy by 0.6 eV. Rao and Srivastava [26] gave a value of $2.6 \times 10^{-20} \text{ cm}^2$ for the cross section of this ion at the maximum of the third peak at 11.5 eV in Fig. 5. Surprisingly, the data of Rao and Srivastava for this fragment negative ion are much lower (at the peaks located at 4.7 eV and 11.5 eV by almost a factor of 10) than the other two sets of measurements. The solid line in Fig. 5 is our suggested cross section, $\sigma_{da,F_2^-}(\epsilon)$, for this ion and was obtained by considering all three sets of measurements.

2.1.5. F^-

The F^- ion is the predominant fragment negative ion produced by dissociative electron attachment to SF_6 at ambient temperature at electron energies above ~ 2.5 eV. Its cross section exhibits maxima at ~ 2.8

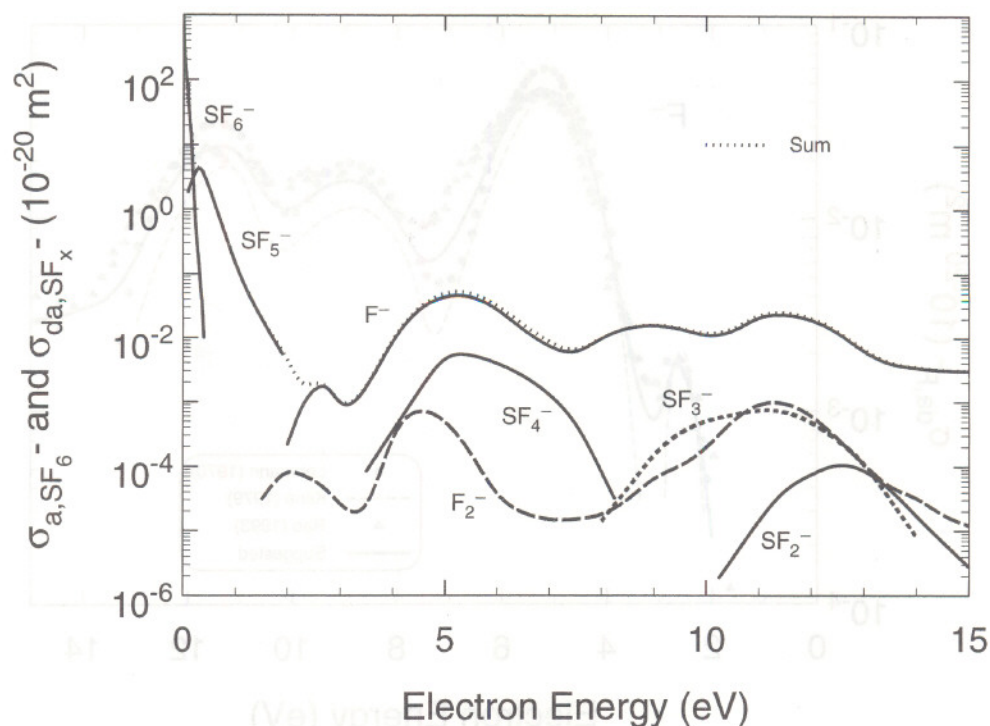


Fig. 7. Recommended or suggested cross sections for the formational SF_6^- [Fig. 3(a)], SF_5^- [Fig. 3(b)], SF_4^- , SF_3^- and SF_2^- (Fig. 4), F_2^- (Fig. 5), and F^- (Fig. 6)., suggested $\sigma_{a,t}(\epsilon)$ (sum of all shown cross sections; see text).

eV, ~ 5.2 eV, ~ 9.1 eV and ~ 11.5 eV (Table 2, Fig. 6). Above ~ 15 eV the data of Rao and Srivastava show formation of F^- possibly via ion-pair processes. The various cross section measurements are shown in Fig. 6. The original data of Rao and Srivastava [26] for this ion were mistakenly reported at values that were low by a factor of ten [109]. The data plotted in Fig. 6 are the original values adjusted upward by a factor of ten. The solid line shown in the figure is the least squares fit to the three sets of data and represents our suggested values for the $\sigma_{\text{da},\text{F}^-}(\epsilon)$.

2.2. Total electron attachment cross section, $\sigma_{a,t}(\epsilon)$, and total dissociative electron attachment cross section, $\sigma_{\text{da},t}(\epsilon)$

In Fig. 7 are plotted the recommended or suggested cross sections for the various negative ions as determined in the preceding sections, namely, for SF_6^-

[Fig. 3(a)], SF_5^- [Fig. 3(b)], SF_4^- , SF_3^- , and SF_2^- (Fig. 4), F_2^- (Fig. 5), and F^- (Fig. 6). The total electron attachment cross section, $\sigma_{a,t}(\epsilon)$, as represented by the sum of all these recommended or suggested cross sections is shown in Fig. 7 by the dotted line, which overlaps the solid line for SF_5^- below ~ 1.5 eV and the solid line for SF_6^- below ~ 0.2 eV. Data taken off this line are listed in Column 2 of Table 3 as our recommended values for the $\sigma_{a,t}(\epsilon)$ of the SF_6 molecule in the energy range 0.0001 eV to 15 eV. The total dissociative electron attachment cross section, $\sigma_{\text{da},t}(\epsilon)$, as represented by the sum of the suggested dissociative electron attachment cross sections for all fragment negative ions is listed in Column 3 of Table 3. The values listed represent our suggested data for the $\sigma_{\text{da},t}(\epsilon)$ of the SF_6 molecule. It is seen from Fig. 7 that beyond ~ 0.3 eV, $\sigma_{\text{da},t}(\epsilon) = \sigma_{a,t}(\epsilon)$, and that $\sigma_{\text{da},t}(\epsilon)$ is dominated by the formation of SF_5^- below ~ 2.0 eV and by the formation of F^- above this energy.

Table 3

Recommended room temperature values of the total electron attachment cross section, $\sigma_{a,t}(\epsilon)$, and the total dissociative electron attachment cross section, $\sigma_{da,t}(\epsilon)$, for SF₆

Electron energy (eV)	$\sigma_{a,t}(\epsilon)$ (10 ⁻²⁰ m ²)	$\sigma_{da,t}(\epsilon)$ (10 ⁻²⁰ m ²)
0.0001	7617	—
0.0002	5283	—
0.0003	4284	—
0.0004	3692	—
0.0005	3280	—
0.0006	2968	—
0.0007	2724	—
0.0008	2529	—
0.0009	2369	—
0.001	2237	—
0.002	1511	—
0.003	1202	—
0.004	993	—
0.005	859	—
0.006	760	—
0.007	683	—
0.008	621	—
0.009	569	—
0.010	526	—
0.015	383	—
0.020	304	—
0.025	257	—
0.030	221	—
0.035	190	—
0.040	171	—
0.045	149	—
0.050	132	—
0.060	109	—
0.070	92.7	—
0.080	82.9	—
0.090	74.3	—
0.10	51.4	1.85
0.12	32.9	2.09
0.14	20.2	2.36
0.15	16.7	2.48
0.16	13.1	2.61
0.18	8.72	2.87
0.20	6.01	3.15
0.22	4.69	3.45
0.25	4.38	3.86
0.28	4.40	4.15
0.30	4.40	4.24
0.35	4.12	4.07
0.40	3.46	3.45
0.45	2.75	2.75
0.50	2.15	2.15
0.60	1.25	1.25
0.70	0.722	0.722
0.80	0.416	0.416

(continued in next column)

Table 3 (continued)

Recommended room temperature values of the total electron attachment cross section, $\sigma_{a,t}(\epsilon)$, and the total dissociative electron attachment cross section, $\sigma_{da,t}(\epsilon)$, for SF₆

Electron energy (eV)	$\sigma_{a,t}(\epsilon)$ (10 ⁻²⁰ m ²)	$\sigma_{da,t}(\epsilon)$ (10 ⁻²⁰ m ²)
0.90	0.245	0.245
1.0	0.147	0.147
1.2	0.060	0.060
1.5	0.020	0.020
2.0	0.0043	0.0043
2.25	0.0020	0.0020
2.5	0.0019	0.0019
2.75	0.0017	0.0017
3.0	0.0010	0.0010
3.5	0.0018	0.0018
4.0	0.0092	0.0092
4.5	0.0290	0.0290
5.0	0.0514	0.0514
5.5	0.0493	0.0493
6.0	0.0317	0.0317
6.5	0.0162	0.0162
7.0	0.0088	0.0088
7.5	0.0066	0.0066
8.0	0.0099	0.0099
8.5	0.0143	0.0143
9.0	0.0159	0.0159
9.5	0.0144	0.0144
10.0	0.0120	0.0120
10.5	0.0142	0.0142
11.0	0.0227	0.0227
11.5	0.0252	0.0252
12.0	0.0206	0.0206
12.5	0.0128	0.0128
13.0	0.0066	0.0066
13.5	0.0041	0.0041
14.0	0.0035	0.0035
14.5	0.0031	0.0031
15.0	0.0030	0.0030

Acknowledgement

We wish to thank Professor H. Hotop for discussions on the electron attachment cross sections at low energies, and for providing parts of Ref. 106 as well as his electronic file on the electron attachment cross section for SF₆⁻ below 0.230 eV.

References

- [1] J.L. Dehmer, A.C. Parr, S. Wallace, D. Dill, Phys. Rev. A 26 (1982) 3283.

- [2] D.M.P. Holland, M.A. MacDonald, P. Baltzer, L. Karlsson, M. Lundqvist, B. Wannberg, W. von Niessen, *Chem. Phys.* 192 (1995) 333.
- [3] K.H. Sze, C.E. Brion, *Chem. Phys.* 140 (1990) 439.
- [4] P.J. Hay, *J. Am. Chem. Soc.* 99 (1977) 1013.
- [5] P.J. Hay, *J. Chem. Phys.* 76 (1982) 502.
- [6] R. Tang, J. Callaway, *J. Chem. Phys.* 84 (1986) 6854.
- [7] M. Klobukowski, Z. Barandiaran, L. Seijo, S. Huzinaga, *J. Chem. Phys.* 86 (1987) 1637.
- [8] J.A.D. Stockdale, R.N. Compton, H.C. Schweinler, *J. Chem. Phys.* 53 (1969) 1502.
- [9] P.S. Drzaic, J.I. Brauman, *Chem. Phys. Lett.* 83 (1981) 508.
- [10] P.S. Drzaic, J.I. Brauman, *J. Am. Chem. Soc.* 104 (1982) 13.
- [11] G.L. Gutsev, Plenum Publishing Corporation, New York, 1992, p. 504 (translated from *Izvestiya Akademii Nauk, Seriya Khimicheskaya*, No. 3, 1992, pp. 641–649).
- [12] G.L. Gutsev, *Int. J. Mass Spectrom. Ion Proc.* 115 (1992) 185.
- [13] K.W. Richman, A. Banerjee, *Int. J. Quantum Chem. Quantum Chem. Symp.* 27, 1993, 759.
- [14] A.A. Christodoulides, D.L. McCorkle, L.G. Christophorou, in *Electron Molecule Interactions and Their Applications*, L.G. Christophorou (Ed.), Academic Press, New York, 1984, Vol. 2, Chap. 6.
- [15] E.P. Grimsrud, S. Chowdhury, P. Kebarle, *J. Chem. Phys.* 83 (1985) 1059.
- [16] E.C.M. Chen, L.-R. Shuie, E.D. D'sa, C.F. Batten, W.E. Wentworth, *J. Chem. Phys.* 88 (1988) 4711.
- [17] E.C.M. Chen, J.R. Wiley, C.F. Batten, W.E. Wentworth, *J. Phys. Chem.* 98 (1994) 88.
- [18] E. Miyoshi, Y. Sakai, S. Miyoshi, *J. Chem. Phys.* 88 (1988) 1470.
- [19] L.G. Christophorou, D.L. McCorkle, J.G. Carter, *J. Chem. Phys.* 54 (1971) 253, Erratum, *J. Chem. Phys.* 57 (1972) 2228.
- [20] L.E. Kline, D.K. Davies, C.L. Chen, P.J. Chantry, *J. Appl. Phys.* 50 (1979) 6789.
- [21] C.L. Chen, P.J. Chantry, *J. Chem. Phys.* 71 (1979) 3897.
- [22] P. Harland, J.C.J. Thynne, *J. Phys. Chem.* 73 (1969) 4031.
- [23] J. Randell, D. Field, S.L. Lunt, G. Mrotzek, J.P. Ziesel, *J. Phys. B* 25 (1992) 2899.
- [24] K. Rohr, *J. Phys. B* 10 (1977) 1175.
- [25] J.L. Dehmer, J. Siegel, D. Dill, *J. Chem. Phys.* 69 (1978) 5205.
- [26] M.V.V.S. Rao, S.K. Srivastava, in: T. Andersen, B. Fastrup, F. Folkmann, H. Knudsen (Eds.), *Proceedings of the 18th International Conference on the Physics of Electronic and Atomic Collisions*, Aarhus, Denmark, July 21–27, 1993, Abstracts of contributed papers, p. 345.
- [27] B. Lehmann, *Z. Naturforsch.* 25A (1970) 1755.
- [28] M. Fenzlaff, R. Gerhard, E. Illenberger, *J. Chem. Phys.* 88 (1988) 149.
- [29] M.S. Dababneh, Y.-F. Hsieh, W.E. Kauppila, C.K. Kwan, S.J. Smith, T.S. Stein, M.N. Uddin, *Phys. Rev. A* 38 (1988) 1207.
- [30] G. Kasperski, P. Mozejko, C. Szymkowski, *Z. Phys. D* 42 (1997) 187.
- [31] N.I. Romanyuk, I.V. Chernyshova, O.B. Shpenik, *Sov. Phys. Tech. Phys.* 29 (1984) 1204.
- [32] R.E. Kennerly, R.A. Bonham, M. McMillan, *J. Chem. Phys.* 70 (1979) 2039.
- [33] K. Rohr, *J. Phys. B* 12 (1979) L185.
- [34] F.A. Gianturco, R.R. Lucchese, N. Sanna, *J. Chem. Phys.* 102 (1995) 5743.
- [35] W.M. Johnstone, W.R. Newell, *J. Phys. B* 24 (1991) 473.
- [36] I. Gyemant, Z. Varga, M.G. Benedict, *Int. J. Quant. Chem.* 17 (1980) 255.
- [37] S. Trajmar, A. Chutjian, *J. Phys. B* 10 (1977) 2943.
- [38] M.G. Benedict, I. Gyemant, *Int. J. Quantum Chem.* 13 (1978) 597.
- [39] D. Edelson, J.E. Griffiths, K.B. McAfee, Jr., *J. Chem. Phys.* 37 (1962) 917.
- [40] R.N. Compton, L.G. Christophorou, G.S. Hurst, P.W. Reinhardt, *J. Chem. Phys.* 45 (1966) 4634.
- [41] P.W. Harland, J.C.J. Thynne, *J. Phys. Chem.* 75 (1971) 3517.
- [42] L.G. Christophorou, *Atomic and Molecular Radiation Physics*, Wiley-Interscience, New York, 1971, ch. 6.
- [43] L.G. Christophorou, *Adv. Electron. Electron Phys.* 46 (1978) 55.
- [44] L.G. Christophorou, D.L. McCorkle, A.A. Christodoulides, in *L.G. Christophorou (Ed.), Electron Molecule Interactions and Their Applications*, Academic Press, New York, 1984, Vol. 1, Ch. 6.
- [45] J.M.S. Henis, C.A. Mabie, *J. Chem. Phys.* 53 (1970) 2999.
- [46] R.W. Odom, D.L. Smith, J.H. Futrell, *J. Phys. B* 8 (1975) 1349.
- [47] M.S. Foster, J.L. Beauchamp, *Chem. Phys. Lett.* 31 (1975) 482.
- [48] C.E. Klots, *J. Chem. Phys.* 46 (1967) 1197.
- [49] P.M. Collins, L.G. Christophorou, E.L. Chaney, J.G. Carter, *Chem. Phys. Lett.* 4 (1970) 646.
- [50] L.G. Christophorou, A. Hadjiantoniou, J.G. Carter, *J. Chem. Soc., Faraday Trans. II*, 69 (1975) 1713.
- [51] C.D. Cooper, R.N. Compton, *J. Chem. Phys.* 59 (1973) 3550.
- [52] J.P. Johnson, D.L. McCorkle, L.G. Christophorou, J.G. Carter, *J. Chem. Soc., Faraday Trans. II*, 71 (1975) 1742.
- [53] S.M. Spyrou, I. Sauers, L.G. Christophorou, *J. Chem. Phys.* 78 (1983) 7200.
- [54] J.E. Delmore, A.D. Appelhans, *J. Chem. Phys.* 84 (1986) 6238.
- [55] S.P. Heneghan, S.W. Benson, *Int. J. Chem. Kinet.* 15 (1983) 109.
- [56] R.K. Curran, *J. Chem. Phys.* 38 (1963) 780.
- [57] R.N. Compton, L.G. Christophorou, R.H. Huebner, *Phys. Lett.* 23 (1966) 656.
- [58] R.N. Compton, R.H. Huebner, P.W. Reinhardt, L.G. Christophorou, *J. Chem. Phys.* 48 (1968) 901.
- [59] L.G. Christophorou, D.L. McCorkle, J.G. Carter, *J. Chem. Phys.* 60 (1974) 3779.
- [60] W.M. Hickam, R.E. Fox, *J. Chem. Phys.* 25 (1956) 642.
- [61] W.M. Hickam, D. Berg, *J. Chem. Phys.* 29 (1958) 517.
- [62] I.S. Buchel'nikova, *Sov. Phys. JETP* 35 (1959) 783.
- [63] R.K. Asundi, J.D. Craggs, *Proc. Phys. Soc.* 83 (1964) 611.
- [64] D. Rapp, D.D. Briglia, *J. Chem. Phys.* 43 (1965) 1480.
- [65] D. Spence, G.J. Schulz, *J. Chem. Phys.* 58 (1973) 1800.

- [66] J.K. Olthoff, R.J. Van Brunt, H.-X. Wan, J.H. Moore, J.A. Tossell, in: L. G. Christophorou, I. Sauers (Eds.), *Gaseous Dielectrics VI*, Plenum Press, New York, 1991, p. 19.
- [67] H.-X. Wan, J.H. Moore, J.K. Olthoff, R.J. Van Brunt, *Plasma Chem. Plasma Proc.* 13 (1993) 1.
- [68] K.S. Gant, L.G. Christophorou, *J. Chem. Phys.* 65 (1976) 2977.
- [69] K.S. Gant, Ph.D. Dissertation, University of Tennessee, 1976.
- [70] R.Y. Pai, L.G. Christophorou, A.A. Christodoulides, *J. Chem. Phys.* 70 (1979) 1169.
- [71] D.L. McCokle, A.A. Christodoulides, L.G. Christophorou, I. Szamrej, *J. Chem. Phys.* 72 (1980) 4049.
- [72] S.R. Hunter, J.G. Carter, L.G. Christophorou, *J. Chem. Phys.* 90 (1989) 4879.
- [73] J.M. Ajello, A. Chutjian, *J. Chem. Phys.* 65 (1976) 5524.
- [74] A. Chutjian, *Phys. Rev. Lett.* 46 (1981) 1511; Erratum, 48 (1982) 289.
- [75] A.J. Chutjian, *J. Phys. Chem.* 86 (1982) 3518.
- [76] A. Chutjian, S.H. Alajajian, O.J. Orient, in: L.G. Christophorou, M.O. Pace (Eds.), *Gaseous Dielectrics IV*, Pergamon Press, New York, 1984, p. 42.
- [77] A. Chutjian, S.H. Alajajian, *Phys. Rev. A* 31 (1985) 2885.
- [78] K. Harth, M.-W. Ruf, H. Hotop, *Z. Phys. D* 14 (1989) 149.
- [79] D. Klar, M.-W. Ruf, H. Hotop, *Aust. J. Phys.* 45 (1992) 263.
- [80] D. Klar, M.-W. Ruf, H. Hotop, *Meas. Sci. Technol.* 5 (1994) 1248.
- [81] D. Klar, M.-W. Ruf, H. Hotop, *Chem. Phys. Lett.* 189 (1992) 448.
- [82] A. Schramm, J.M. Weber, J. Kreil, D. Klar, M.-W. Ruf, H. Hotop, *Phys. Rev. Lett.* 81 (1998) 778.
- [83] W.P. West, G.W. Foltz, F.B. Dunning, C.J. Latimer, R.F. Stebbings, *Phys. Rev. Lett.* 36 (1976) 854.
- [84] G.W. Foltz, C.J. Latimer, G.F. Hildebrandt, F.G. Kellert, K.A. Smith, W.P. West, F.B. Dunning, R.F. Stebbings, *J. Chem. Phys.* 67 (1977) 1352.
- [85] J.P. Astruc, R. Barbé, J.P. Schermann, *J. Phys. B* 12 (1979) L377.
- [86] B.G. Zollars, K.A. Smith, F.B. Dunning, *J. Chem. Phys.* 81 (1984) 3158.
- [87] B.G. Zollars, C. Higgs, F. Lu, C.W. Walter, L.G. Gray, K.A. Smith, F.B. Dunning, R.F. Stebbings, *Phys. Rev. A* 32 (1985) 3330.
- [88] B.G. Zollars, C.W. Walter, F. Lu, C.B. Johnson, K.A. Smith, F.B. Dunning, *J. Chem. Phys.* 84 (1986) 5589.
- [89] F.B. Dunning, *J. Phys. Chem.* 91 (1987) 2244.
- [90] I.M. Beterov, G.L. Vasilenko, I.I. Riabtsev, B.M. Smirnov, N.V. Fatayev, *Z. Phys. D* 6 (1987) 55.
- [91] Z. Zheng, K.A. Smith, F.B. Dunning, *J. Chem. Phys.* 89 (1988) 6295.
- [92] H.S. Carman, Jr., C.E. Klots, R.N. Compton, *J. Chem. Phys.* 90 (1989) 2580.
- [93] A. Pesnelle, C. Ronge, M. Perdrix, G. Watel, *Phys. Rev. A* 42 (1990) 273.
- [94] X. Ling, B.G. Lindsay, K.A. Smith, F.B. Dunning, *Phys. Rev. A* 45 (1992) 242.
- [95] R.A. Popple, M.A. Durham, R.W. Marawar, B.G. Lindsay, K.A. Smith, F.B. Dunning, *Phys. Rev. A* 45 (1992) 247.
- [96] A. Pesnelle, M. Perdrix, G. Watel, *J. Chem. Phys.* 96 (1992) 4303.
- [97] D. Klar, B. Mirbach, H.J. Korsch, M.-W. Ruf, H. Hotop, *Z. Phys. D* 31 (1994) 235.
- [98] M.T. Frey, S.B. Hill, K.A. Smith, F.B. Dunning, I.I. Fabrikant, *Phys. Rev. Lett.* 75 (1995) 810.
- [99] F.B. Dunning, *J. Phys. B* 28 (1995) 1645.
- [100] R.W. Crompton, G.N. Haddad, *Aust. J. Phys.* 36 (1983) 15.
- [101] H. Hotop, D. Klar, J. Kreil, M.-W. Ruf, A. Schramm, J.M. Weber, in: L.J. Dubé, J.B.A. Mitchell, J.W. McConkey, C.E. Brion (Eds.), *The Physics of Electronic and Atomic Collisions*, AIP Conference Proceedings, vol. 360, AIP Press, Woodbury, New York, 1995, p. 267.
- [102] Z.L. Petrovic, R.W. Crompton, *J. Phys. B* 18 (1985) 2777.
- [103] E.P. Wigner, *Phys. Rev.* 73 (1948) 1002.
- [104] A. Chutjian, Private communication, 1999.
- [105] S. Matejcik, P. Eichberger, B. Plunger, A. Kiendler, A. Stamatovic, T.D. Märk, *Int. J. Mass Spectrom. Ion Processes* 144 (1995) L13.
- [106] A. Schramm, Dissertation, University of Kaiserslautern, 1988.
- [107] H. Hotop, Private communication, 2000.
- [108] D. Rapp, P. Englander-Golden, *J. Chem. Phys.* 43 (1965) 1464.
- [109] M.V.V.S. Rao, Private communication, 1999.

